Contents

List of algorithms

Chapter 13

Mathematical morphology

13.1 Basic morphological concepts

- started to develop in the late 1960s
- based on the algebra of non-linear operators
- operates on object shape
- in some respects supersedes the linear algebraic system of convolution
- can be used for:
  - pre-processing
  - segmentation using object shape
  - object quantification
  - in some ways works better and faster than standard approaches
- slightly different algebra may be confusing

Morphological operations use:

- Image pre-processing (noise filtering, shape simplification).
- Enhancing object structure (skeletonizing, thinning, thickening, convex hull, object marking).
- Segmenting objects from the background.
- Quantitative description of objects (area, perimeter, projections, Euler-Poincaré characteristic).

- initial assumption — real images can be modeled using **point sets** of any dimension
- e.g., N-dimensional Euclidean space
- Euclidean 2D space $\mathcal{E}^2$ and its system of subsets is a natural domain for planar shape description
- Set **difference**

$$X \setminus Y = X \cap Y^c \,. \tag{13.1}$$

- starting with binary images – point set – subsets of 2D space of all integers, $\mathcal{Z}^2$
- point represented by a pair of integers that give co-ordinates
- unit length = sampling period in each direction
- suitable for both rectangular and hexagonal grids
- rectangular grid assumed from now forward

- binary image – 2D point set
- object points = set X (pixel value = 1)
- complement set X^c = background (pixel value = 0)
- diagonal cross = origin – co-ordinates $(0, 0)$

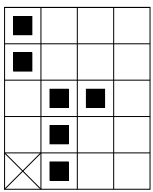

Figure 13.1: A point set example.

- **morphological transformation** Ψ = relation of the image (point set X) with a (small) point set B
- B called a **structuring element**
- B expressed with respect to a local origin $\mathcal{O}$ (called representative point)

- applying morphological transformation $\Psi(X)$ to image X
- structuring element B moves systematically across entire image

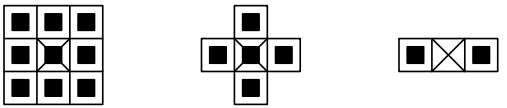

Figure 13.2: Typical structuring elements.

- **duality** – for each morphological transformation $\Psi(X)$ exists a dual transformation $\Psi^*(X)$

$$\Psi(X) = \left(\Psi^*(X^c)\right)^c \tag{13.2}$$

- **translation** of point set X by vector h – denoted by X_h

$$X_h = \left\{p \in \mathcal{E}^2 \ , \ p = x + h \text{ for some } x \in X\right\} . \tag{13.3}$$

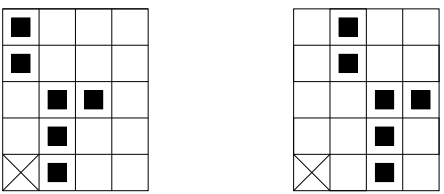

Figure 13.3: Translation by a vector.

13.2 Four morphological principles

- morphological transformations may be restricted by several constraints — four morphological principles
- these concepts may be difficult to understand
- understanding is not essential to comprehension
- MM with quantified results – two main steps:
  - (a) geometrical transformation
  - (b) actual measurement
- morphological operator = composition of mapping Ψ (or geometrical transformation) followed by a measure μ which is a mapping $Z \times \ldots \times Z \longrightarrow R$
- geometrically transformed set $\Psi(X)$ can be the boundary
- measure $\mu[\Psi(X)]$ yields a number (weight, surface area, volume, etc.)
- A morphological transformation is called **quantitative** if and only if it satisfies four basic principles [Serra 82]

– Compatibility with translation:
let transformation Ψ depend on position of origin $\mathcal{O}$ ... $\Psi_{\mathcal{O}}$
if all points are translated by the vector $-h$, it is expressed as Ψ_{-h}
compatibility with translation principle:

$$\Psi_{\mathcal{O}}(X_h) = \big(\Psi_{-h}(X)\big)_h \tag{13.4}$$

if Ψ does not depend on position of origin $\mathcal{O}$, principle reduces to invariance under translation

$$\Psi(X_h) = \big(\Psi(X)\big)_h \,. \tag{13.5}$$

– Compatibility with change of scale:
let $\lambda\, X$ represent the homothetic scaling of a point set X
(i.e., co-ordinates of each point of the set are multiplied by some positive constant λ) – change of scale
let Ψ_λ denote transformation that depends on the positive parameter λ (change of scale)
Compatibility with change of scale:

$$\Psi_\lambda(X) = \lambda\, \Psi\left(\frac{1}{\lambda}\, X\right) \,. \tag{13.6}$$

if Ψ does not depend on the scale λ, then compatibility with change of scale reduces to invariance to change of scale

$$\Psi(\lambda\, X) = \lambda\, \Psi(X) \,. \tag{13.7}$$

– Local knowledge:
considers situation in which only a part of a larger structure can be examined—this is always the case in reality
morphological transformation Ψ satisfies the *local knowledge principle* if for any bounded point set Z' in transformation $\Psi(X)$ there exists a bounded set Z, knowledge of which is sufficient to provide Ψ

$$\big(\Psi(X \cap Z)\big) \cap Z' = \Psi(X) \cap Z' \,. \tag{13.8}$$

– Upper semi-continuity:
morphological transformation does not exhibit any abrupt changes – precise explanation needs many concepts from topology and is given in [Serra 82].

13.3 Binary dilation and erosion

13.3.1 Dilation

- **dilation** $\oplus$ combines two sets using vector addition
  $\big($or Minkowski set addition, e.g., $(a,b)+(c,d)=(a+c,b+d)\big)$
- dilation $X \oplus B$ is point set of all possible vector additions of pairs of elements, one from each of the sets X and B

$$X \oplus B = \left\{ p \in \mathcal{E}^2 : \; p = x + b, \; x \in X \text{ and } b \in B \right\}. \tag{13.9}$$

$$\begin{aligned} X &= \left\{(1,0),(1,1),(1,2),(2,2),(0,3),(0,4)\right\}, \\ B &= \left\{(0,0),(1,0)\right\}, \\ X \oplus B &= \left\{(1,0),(1,1),(1,2),(2,2),(0,3),(0,4),(2,0),(2,1),(2,2),(3,2),(1,3),(1,4)\right\}. \end{aligned}$$

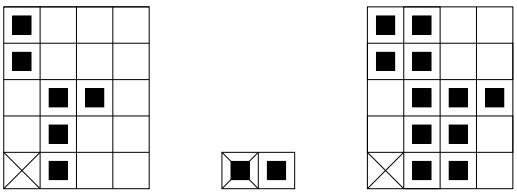

Figure 13.4: Dilation.

- structuring element 3×3 (Figure 13.2a)
- dilation (isotropic expansion) – Figure 13.5.
- called *fill* or *grow*

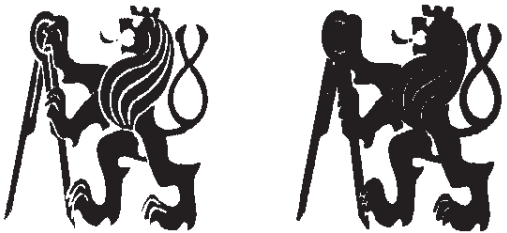

Figure 13.5: Dilation as isotropic expansion.

Dilation properties:
The dilation operation is commutative

$$X \oplus B = B \oplus X \tag{13.10}$$

and is also associative

$$X \oplus (B \oplus D) = (X \oplus B) \oplus D\,. \tag{13.11}$$

Dilation may be expressed as a union of shifted point sets

$$X \oplus B = \bigcup_{b \in B} X_b \tag{13.12}$$

and is invariant to translation

$$X_h \oplus B = (X \oplus B)_h \, . \tag{13.13}$$

- Equations (13.12) and (13.13) show importance of shifts in speeding up implementation of dilation
- this holds for implementations of binary morphology on serial computers in general
- one processor word represents several pixels (e.g., 32 for a 32-bit processor), and shift or addition corresponds to a single instruction
- shifts may also be easily implemented as delays in a pipeline parallel processor

- Dilation is an **increasing** transformation:

$$\text{If } X \subseteq Y \text{ then } X \oplus B \subseteq Y \oplus B\,. \tag{13.14}$$

- used to fill small holes and narrow gulfs in objects

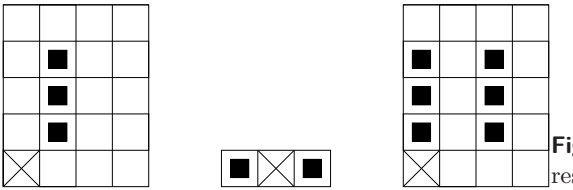

Figure 13.6: Dilation where the representative point is not a member of the structuring element.

13.3.2 Erosion

- **Erosion** $\ominus$ combines two sets using vector subtraction of set elements
- dual operator of dilation
- neither erosion nor dilation are invertible transformation

$$X \ominus B = \left\{ p \in \mathcal{E}^2 : \; p = x + b \in X \text{ for every } b \in B \right\}. \tag{13.15}$$

This formula says that every point p from the image is tested; the result of the erosion is given by those points p for which all possible $p + b$ are in X

$$\begin{aligned} X &= \left\{ (1,0), (1,1), (1,2), (0,3), (1,3), (2,3), (3,3), (1,4) \right\}, \\ B &= \left\{ (0,0), (1,0) \right\}, \\ X \ominus B &= \left\{ (0,3), (1,3), (2,3) \right\}. \end{aligned}$$

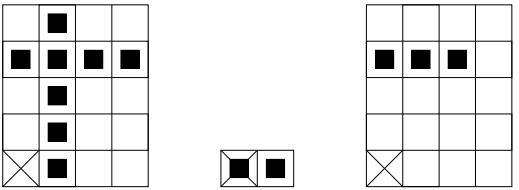

Figure 13.7: Erosion.

Figure 13.8: Erosion as isotropic shrink.

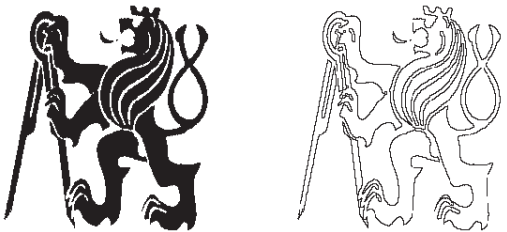

Figure 13.9: Contours obtained by subtraction of an eroded image from an original (left).

Erosion is used to simplify the structure of an object—objects or their parts with width equal to one will disappear

It might thus decompose complicated objects into several simpler ones

There is an equivalent definition of erosion [Matheron 75]. Recall that B_p denotes B translated by p

$$X \ominus B = \left\{ p \in \mathcal{E}^2 : \; B_p \subseteq X \right\} . \tag{13.16}$$

- erosion – another way of understanding – structuring element B slides across the image X
  - if B translated by vector p is contained in the image X
  - then point corresponding to the representative point of B belongs to erosion $X \ominus B$
- image X eroded by the structuring element B ... intersection of all translations of the image X by vector $-b \in B$

$$X \ominus B = \bigcap_{b \in B} X_{-b} \tag{13.17}$$

- Erosion is translation invariant

$$X_h \ominus B = (X \ominus B)_h , \tag{13.18}$$
$$X \ominus B_h = (X \ominus B)_{-h} , \tag{13.19}$$

- Erosion is increasing transformation

$$\text{If } X \subseteq Y \text{ then } X \ominus B \subseteq Y \ominus B . \tag{13.20}$$

- B, D structuring elements, D contained in B
  then erosion by B is more aggressive than by D
  = if $D \subseteq B$, then $X \ominus B \subseteq X \ominus D$
- this enables ordering of erosions according to structuring elements of similar shape but different sizes

- Let $\breve{B}$ be **symmetrical set** to B
- called the **transpose** [Serra 82] or **rational set** with respect to $\mathcal{O}$

$$\breve{B} = \{-b : \ b \in B\} \, . \tag{13.21}$$

- For example

$$\begin{aligned} B &= \big\{(1,2),(2,3)\big\} \, , \\ \breve{B} &= \big\{(-1,-2),(-2,-3)\big\} \, . \end{aligned} \tag{13.22}$$

- Erosion and dilation are dual transformations

$$(X \ominus Y)^C = X^C \oplus \breve{Y} \, . \tag{13.23}$$

- Differences between erosion and dilation
  (Erosion (in contrast to dilation) is not commutative)

$$X \ominus B \neq B \ominus X \, . \tag{13.24}$$

- combined properties of erosion and intersection

$$\begin{aligned} (X \cap Y) \ominus B &= (X \ominus B) \cap (Y \ominus B) \, , \\ B \ominus (X \cap Y) &\supseteq (B \ominus X) \cup (B \ominus Y) \, . \end{aligned} \tag{13.25}$$

- image intersection and dilation cannot be interchanged
  dilation of the intersection of two images is contained in the intersection of their dilations

$$(X \cap Y) \oplus B = B \oplus (X \cap Y) \subseteq (X \oplus B) \cap (Y \oplus B)\,. \tag{13.26}$$

- order of erosion may be interchanged with set union
  $\Rightarrow$ enables the structuring element to be decomposed into a union of simpler structuring elements

$$\begin{aligned} B \oplus (X \cup Y) &= (X \cup Y) \oplus B = (X \oplus B) \cup (Y \oplus B)\,, \\ (X \cup Y) \ominus B &\supseteq (X \ominus B) \cup (Y \ominus B)\,, \\ B \ominus (X \cup Y) &= (X \ominus B) \cap (Y \ominus B)\,. \end{aligned} \tag{13.27}$$

- Successive dilation (respectively, erosion) of image X first by the structuring element B and then by the structuring element D is equivalent to dilation (erosion) of the image X by $B \oplus D$

$$\begin{aligned} (X \oplus B) \oplus D &= X \oplus (B \oplus D)\,, \\ (X \ominus B) \ominus D &= X \ominus (B \oplus D)\,. \end{aligned} \tag{13.28}$$

13.3.3 Hit-or-miss transformation

- Hit-or-miss transformation — finding local patterns of pixels
- *local* with respect to size of structuring element
- variant of template matching = finds collections of pixels with certain shape properties (such as corners, or border points)
- may be used for thinning and thickening of objects
- So far – points were tested for their membership
- points can be tested whether they do not belong to X
- ... pair of disjoint sets $B = (B_1, B_2)$ ... **composite structuring element**

- **hit-or-miss** transformation $\otimes$ defined as

$$X \otimes B = \left\{ x : \; B_1 \subset X \text{ and } B_2 \subset X^c \right\} . \tag{13.29}$$

- for point x to be in resulting set, two conditions must be fulfilled simultaneously:
  - part B_1 of composite structuring element with representative point at x must be contained in X
  - part B_2 of composite structuring element must be in X^c
- hit-or-miss transformation = binary matching between image X and element (B_1, B_2)
- hit or miss can be expressed using erosions and dilations

$$X \otimes B = (X \ominus B_1) \cap (X^c \ominus B_2) = (X \ominus B_1) \setminus (X \oplus \breve{B}_2) . \tag{13.30}$$

13.3.4 Opening and closing

- Erosion and dilation are not inverse transformations
- Erosion followed by dilation – **opening** $X \circ B$

$$X \circ B = (X \ominus B) \oplus B \,. \tag{13.31}$$

- Dilation followed by erosion – **closing** $X \bullet B$

$$X \bullet B = (X \oplus B) \ominus B \,. \tag{13.32}$$

- if image X is unchanged by opening with structuring element B = it is *open with respect to* B
- if image X is unchanged by closing with B, it is *closed with respect to* B
- isotropic opening/closing eliminates specific image details smaller than the structuring element — global shape not distorted
- closing connects objects that are close to each other, fills small holes, smoothes outline by filling up narrow gulfs

Figure 13.10: Opening (original on the left).

Figure 13.11: Closing (original on the left).

- opening and closing are invariant to translation of structuring element
- opening and closing are increasing transformations
- opening is anti-extensive ($X \circ B \subseteq X$)
- closing is extensive ($X \subseteq X \bullet B$)
- opening and closing are dual transformations

$$(X \bullet B)^C = X^C \circ \breve{B}\,. \tag{13.33}$$

- iteratively used openings and closings are **idempotent** = reapplication of these transformations does not change the previous result

$$X \circ B = (X \circ B) \circ B\,, \tag{13.34}$$

$$X \bullet B = (X \bullet B) \bullet B\,. \tag{13.35}$$

13.4 Gray-scale dilation and erosion

- Binary morphological operations are extendible to gray-scale images using the 'min' and 'max' operations.
- Erosion – assigns to each pixel minimum value in a neighborhood of corresponding pixel in input image
  - structuring element is richer than in binary case
  - structuring element is a function of two variables, specifies desired local gray-level property
  - value of structuring element is added when maximum is calculated in the neighborhood
- Dilation – assigns maximum value in neighborhood of corresponding pixel in input image
  - value of structuring element is subtracted when minimum is calculated in the neighborhood

- Such extension permits **topographic view** of gray-scale images
  - gray-level is interpreted as height of a particular location of a hypothetical landscape
  - light and dark spots in the image correspond to hills and valleys
  - such morphological approach permits the location of global properties of the image
    valleys
    mountain ridges (crests)
    watersheds

Gray-scale dilation and erosion
– use concept of **umbra** and **top of the point set**
Gray-scale dilation is expressed as the dilation of umbras.

13.4.1 Top surface, umbra, and gray-scale dilation and erosion

- point set $A \subset \mathcal{E}^n$
- first $(n-1)$ co-ordinates ... spatial domain
- n^{th} co-ordinate ... function value (brightness)
- The **top surface** of set A = function defined on the $(n-1)$-dimensional support
- for each $(n-1)$-tuple, top surface is the highest value of the last co-ordinate of A for each $(n-1)$-tuple
- if A is Euclidean, highest value means supremum

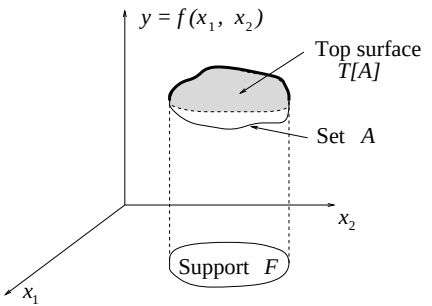

Figure 13.12: Top surface of the set A corresponds to maximal values of the function $f(x_1, x_2)$.

- $A \subseteq \mathcal{E}^n$
- support $F = \{x \in \mathcal{E}^{n-1} \text{ for some } y \in \mathcal{E},\ (x, y) \in A\}$
- **top surface** $T[A]$ is mapping $F \to \mathcal{E}$

$$T[A](x) = \max\left\{y,\ (x, y) \in A\right\} \tag{13.36}$$

- **umbra** of function f is defined on some subset F (support) of $(n-1)$-dimensional space
- umbra – region of complete shadow when obstructing light by non-transparent object
- umbra of f ... set consisting of top surface of f and everything below it

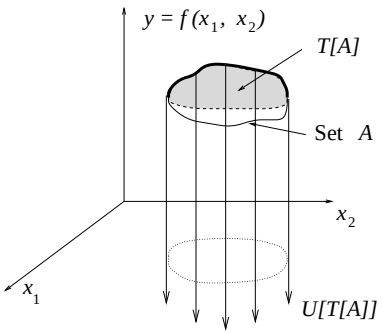

Figure 13.13: Umbra of the top surface of a set is the whole subspace below it.

- let $F \subseteq \mathcal{E}^{n-1}$ and $f : F \to \mathcal{E}$
- **umbra** $U[f]$, $U[f] \subseteq F \times \mathcal{E}$

$$U[f] = \left\{(x, y) \in F \times \mathcal{E},\ y \leq f(x)\right\}. \tag{13.37}$$

- umbra of an umbra of f is an umbra.

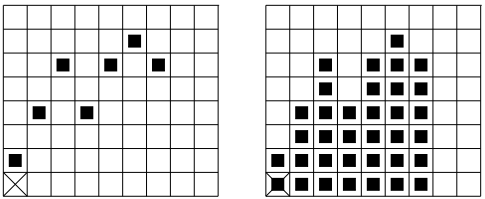

Figure 13.14: Example of a 1D function (left) and its umbra (right).

Gray-scale Dilation

- gray-scale dilation of two functions
  ... top surface of the dilation of their umbras
- let $F, K \subseteq \mathcal{E}^{n-1}$ and $f : F \to \mathcal{E}$ and $k : K \to \mathcal{E}$
- **dilation** $\oplus$ of f by k, $f \oplus k : F \oplus K \to \mathcal{E}$ is defined by

$$f \oplus k = T\big\{U[f] \oplus U[k]\big\} \,. \tag{13.38}$$

- $\oplus$ on the left-hand side is dilation in the gray-scale image domain
- $\oplus$ on the right-hand side is dilation in the binary image
- no new symbol introduced
- the same applies to erosion $\ominus$ later
- similar to binary dilation
  one function f represents image
  second function k represents structuring element

- figure shows discretized function k ... structuring element

Figure 13.15: A structuring element: 1D function (left) and its umbra (right).

- figure 13.16 shows dilation of umbra of f by umbra of k

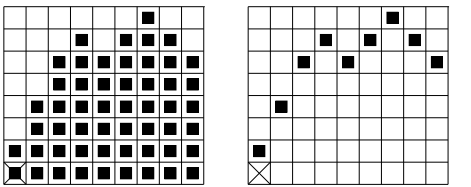

Figure 13.16: 1D example of gray-scale dilation. The umbras of the 1D function f and structuring element k are dilated first, $U[f] \oplus U[k]$. The top surface of this dilated set gives the result, $f \oplus k = T\big[U[f] \oplus U[k]\big]$.

- This explains what gray-scale dilation means
- does not give a reasonable algorithm for actual computations in hardware
- computationally plausible way to calculate dilation ... taking the maximum of a set of sums:

$$(f \oplus k)(x) = \max\left\{f(x-z) + k(z),\ z \in K,\ x - z \in F\right\}. \tag{13.39}$$

- computational complexity is the same as for convolution in linear filtering, where a summation of products is performed

Gray-scale Erosion

- definition of **gray-scale erosion** is analogous to gray-scale dilation.
- gray-scale erosion of two functions (point sets)
  1. Takes their umbras.
  2. Erodes them using binary erosion.
  3. Gives the result as the top surface.
- let $F, K \subseteq \mathcal{E}^{n-1}$ and $f : F \to \mathcal{E}$ and $k : K \to \mathcal{E}$
- **erosion** $\ominus$ of f by k, $f \ominus k : F \ominus K \to \mathcal{E}$

$$f \ominus k = T\big\{U[f] \ominus U[k]\big\} . \tag{13.40}$$

- to decrease computational complexity, the actual computations performed as the minimum of a set of differences (notice similarity to correlation)

$$(f \ominus k)(x) = \min_{z \in K} \big\{ f(x+z) - k(z) \big\} . \tag{13.41}$$

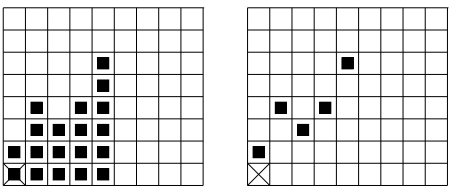

Figure 13.17: 1D example of gray-scale erosion. The umbras of 1D function f and structuring element k are eroded first, $U[f] \ominus U[k]$. The top surface of this eroded set gives the result, $f \ominus k = T\big[U[f] \ominus U[k]\big]$.

Example

- microscopic image of cells corrupted by noise
- aim is to reduce noise and locate individual cells
- 3×3 structuring element used for erosion/dilation
- individual cells can be located by the reconstruction operation (Section 13.5.4) – original image is used as a mask and the dilated image in Figure 13.18c is an input for reconstruction
- black spots in (d) panel depict cells

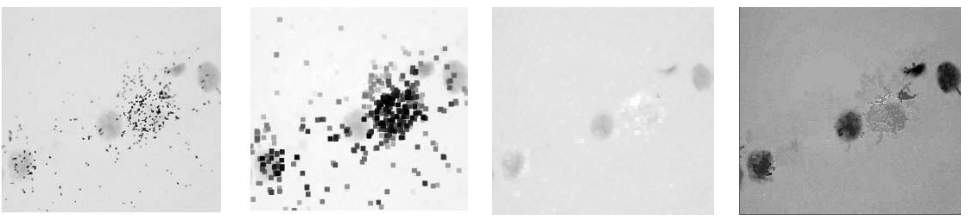

Figure 13.18: Morphological pre-processing: (a) cells in a microscopic image corrupted by noise; (b) eroded image; (c) dilation of (b), the noise has disappeared; (d) reconstructed cells. *Courtesy of P. Kodl, Rockwell Automation Research Center, Prague, Czech Republic.*

13.4.2 Opening and Closing

Gray-scale opening and closing

- defined as in binary morphology
- **Gray-scale opening** $f \circ k = (f \ominus k) \oplus k$
- **gray-scale closing** $f \bullet k = (f \oplus k) \ominus k$
- **duality** between opening and closing is expressed as ($\breve{k}$ means transpose = symmetric set)

$$-(f \circ k)(x) = \big((-f) \bullet \breve{k}\big)(x)\,. \tag{13.42}$$

- opening of f by structuring element k can be interpreted as sliding k on the landscape f
- position of all highest points reached by some part of k during the slide gives the opening,
- similar interpretation exists for erosion
- Gray-scale opening and closing often used to extract parts of a gray-scale image with given shape and gray-scale structure

13.4.3 Top hat transformation

- simple tool for segmenting objects in gray-scale images that differ in brightness from background
  even when background is uneven
- top-hat transform superseded by watershed segmentation for more complicated backgrounds
- gray-level image X, structuring element K
- residue of opening as compared to original image $X \setminus (X \circ K)$ is **top hat transformation**
- good tool for extracting light (or dark) objects on dark (light) possibly slowly changing background
- parts of image that cannot fit into structuring element K are removed by opening
- Subtracting opened image from original – removed objects stand out clearly
- actual segmentation performed by simple thresholding

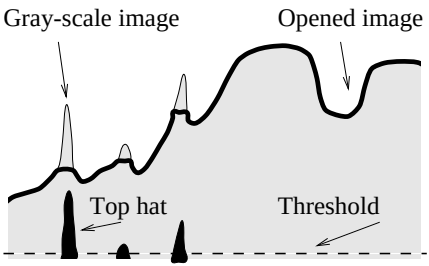

Figure 13.19: The top hat transform permits the extraction of light objects from an uneven background.

Example from visual industrial inspection

- glass capillaries for mercury maximal thermometers had the following problem: thin glass tube should be narrowed in one particular place to prevent mercury falling back when the temperature decreases from the maximal value
  done by using a narrow gas flame and low pressure in the capillary
- capillary is illuminated by a collimated light beam—when the capillary wall collapses due to heat and low pressure, an instant specular reflection is observed and serves as a trigger to cover the gas flame
- Originally, machine was controlled by a human operator who looked at the tube image projected optically on the screen; the gas flame was covered when the specular reflection was observed
- task had to be automated and the trigger signal obtained from a digitized image
- $\Rightarrow$ specular reflection is detected by a morphological procedure

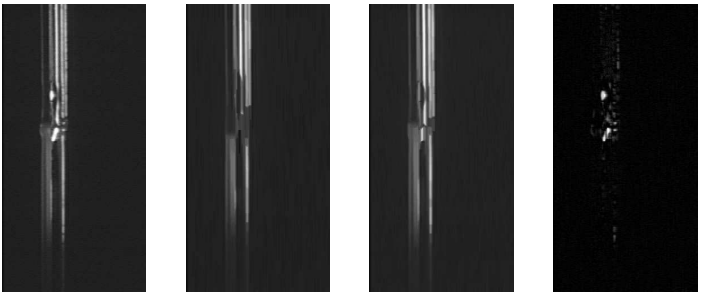

(a) (b) (c) (d)

Figure 13.20: An industrial example of gray-scale opening and top hat segmentation, i.e., image-based control of glass tube narrowing by gas flame. (a) Original image of the glass tube, 512×256 pixels. (b) Erosion by a one-pixel-wide vertical structuring element 20 pixels long. (c) Opening with the same element. (d) Final specular reflection segmentation by the top hat transformation. *Courtesy of V. Smutný, R. Šára, CTU Prague, P. Kodl, Rockwell Automation Research Center, Prague, Czech Republic.*

13.5 Skeletons and object marking

13.5.1 Homotopic transformations

- transformation is homotopic if it does not change the continuity relation between regions and holes in the image.
- this relation expressed by homotopic tree
  - its root ... image background
  - first-level branches ... objects (regions)
  - second-level branches ... holes
  - etc.
- transformation is homotopic if it does not change homotopic tree

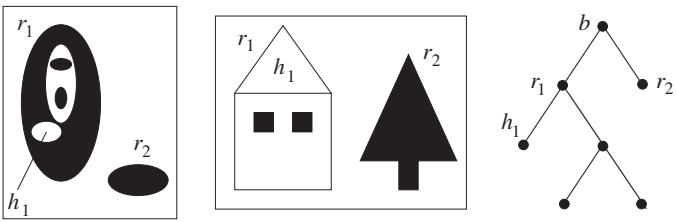

Figure 13.21: The same homotopic tree for two different images.

13.5.2 Skeleton, maximal ball

- skeletonization = **medial axis transform**
- 'grassfire' scenario
- A grassfire starts on the entire region boundary at the same instant – propagates towards the region interior with constant speed
- **skeleton** $S(X)$ ... set of points where two or more firefronts meet

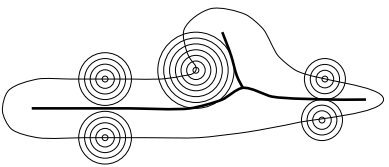

Figure 13.22: Skeleton as points where two or more firefronts of grassfire meet.

- Formal definition of skeleton based on maximal ball concept
- **ball** $B(p, r)$, $r \geq 0$ ... set of points with distances d from center $\leq r$
- ball B included in a set X is **maximal** if and only if there is no larger ball included in X that contains B

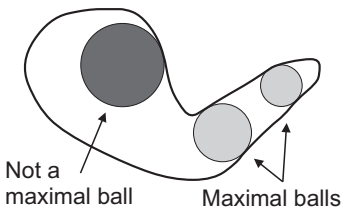

Figure 13.23: Ball and two maximal balls in a Euclidean plane.

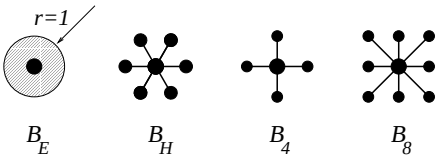

Figure 13.24: Unit-size disk for different distances, from left side: Euclidean distance, 6-, 4-, and 8-connectivity, respectively.

- plane $\mathcal{R}^2$ with usual Euclidean distance gives unit ball B_E
- three distances and balls are often defined in the discrete plane $\mathcal{Z}^2$
- if support is a square grid, two unit balls are possible:
  B_4 for 4-connectivity
  B_8 for 8-connectivity
- **skeleton by maximal balls** $S(X)$ of a set $X \subset \mathcal{Z}^2$ is the set of centers p of maximal balls

$$S(X) = \left\{ p \in X : \exists r \geq 0,\ B(p,r) \text{ is a maximal ball of } X \right\}.$$

- this definition of skeleton has intuitive meaning in Euclidean plane
- skeleton of a disk reduces to its center
- skeleton of a stripe with rounded endings is a unit thickness line at its center
- etc.

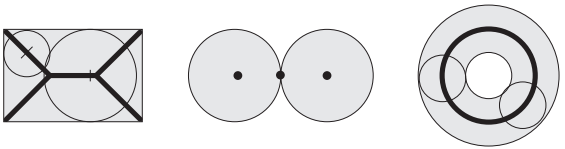

Figure 13.25: Skeletons of rectangle, two touching balls, and a ring.

- skeleton by maximal balls – two unfortunate properties
- does not necessarily preserve homotopy (connectivity)
- some of skeleton lines may be wider than one pixel
- skeleton is often substituted by sequential homotopic thinning that does not have these two properties
- dilation can be used in any of the discrete connectivities to create balls of varying radii
- nB = ball of radius n

$$n\,B = B \oplus B \oplus \ldots \oplus B\,. \tag{13.43}$$

- skeleton by maximal balls ... union of the residues of opening of set X at all scales

$$S(X) = \bigcup_{n=0}^{\infty} \Big((X \ominus nB) \setminus (X \ominus nB) \circ B \Big)\,. \tag{13.44}$$

- trouble is that resulting skeleton is completely disconnected and this property is not useful in many applications

- **homotopic skeletons** that preserve connectivity are preferred

13.5.3 Thinning, thickening, and homotopic skeleton

- hit-or-miss transformation can be used for **thinning** and **thickening** of point sets
- image X and a composite structuring element $B = (B_1, B_2)$
- notice that B here is not a ball
- *thinning*

$$X \oslash B = X \setminus (X \otimes B) \tag{13.45}$$

- *thickening*

$$X \odot B = X \cup (X \otimes B)\,. \tag{13.46}$$

- thinning – part of object boundary is subtracted by set difference operation
- thickening – part of background boundary is added
- Thinning and thickening are dual transformations

$$(X \odot B)^c = X^c \oslash B\,, \qquad B = (B_2, B_1)\,. \tag{13.47}$$

- Thinning and thickening often used sequentially
- Let $\{B_{(1)}, B_{(2)}, B_{(3)}, \ldots, B_{(n)}\}$ denote a sequence of composite structuring elements $B_{(i)} = (B_{i_1}, B_{i_2})$
- **Sequential thinning** – sequence of n structuring elements

$$X \oslash \{B_{(i)}\} = \Big(\big((X \oslash B_{(1)}) \oslash B_{(2)}\big) \ldots \oslash B_{(n)}\Big) \tag{13.48}$$

- **sequential thickening**

$$X \odot \{B_{(i)}\} = \Big(\big((X \odot B_{(1)}) \odot B_{(2)}\big) \ldots \odot B_{(n)}\Big) . \tag{13.49}$$

- several sequences of structuring elements $\{B_{(i)}\}$ are useful in practice
- e.g., permissible rotation of structuring element in digital raster (e.g., hexagonal, square, or octagonal)
- These sequences are called the **Golay alphabet**
- composite structuring element – expressed by a single matrix
- "one" means that this element belongs to B_1 (it is a subset of objects in the hit-or-miss transformation)
- "zero" belongs to B_2 and is a subset of the background
- $*$ ... element not used in matching process = its value is not significant

- Thinning and thickening sequential transformations converge to some image—the number of iterations needed depends on the objects in the image and the structuring element used
- if two successive images in the sequence are identical, the thinning (or thickening) is stopped

Sequential thinning by structuring element L

- thinning by L serves as homotopic substitute of the skeleton;
- final thinned image consists only of lines of width one and isolated points
- structuring element L from the Golay alphabet is given by

$$L_1 = \begin{bmatrix} 0 & 0 & 0 \\ * & 1 & * \\ 1 & 1 & 1 \end{bmatrix}, \quad L_2 = \begin{bmatrix} * & 0 & 0 \\ 1 & 1 & 0 \\ * & 1 & * \end{bmatrix}, \quad \ldots \tag{13.50}$$

- (The other six elements are given by rotation).

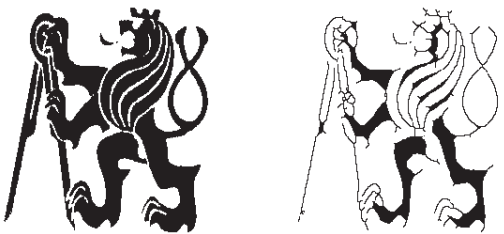

Figure 13.26: Sequential thinning using element L after five iterations.

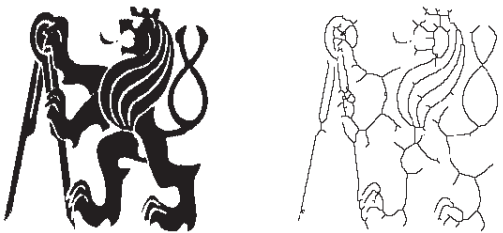

Figure 13.27: Homotopic substitute of the skeleton (element L).

Sequential thinning by structuring element E

- Assume that homotopic substitute by element L was found
- such a skeleton is usually jagged (sharp points on outline of the object)
- possible to 'smooth' the skeleton by sequential thinning by structuring element E
- after n iterations, several points (number depends on n) from the lines of width one (and isolated points as well) are removed from free ends
- if thinning by element E is performed until the image does not change
- $\Rightarrow$ only closed contours remain
- structuring element E from the Golay alphabet is given again by rotated masks,

$$E_1 = \begin{bmatrix} * & 1 & * \\ 0 & 1 & 0 \\ 0 & 0 & 0 \end{bmatrix}, \quad E_2 = \begin{bmatrix} 0 & * & * \\ 0 & 1 & 0 \\ 0 & 0 & 0 \end{bmatrix}, \quad \ldots \tag{13.51}$$

- other elements M, D, C exist in the Golay alphabet [Golay 69] – not much used in practice at present, and other morphological algorithms are used instead to find skeletons, convex hulls, and homotopic markers.

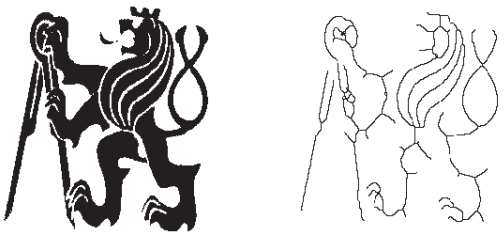

Figure 13.28: Five iterations of sequential thinning by element E.

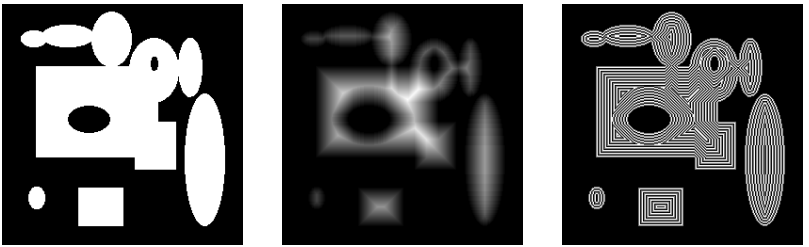

(a) (b) (c)

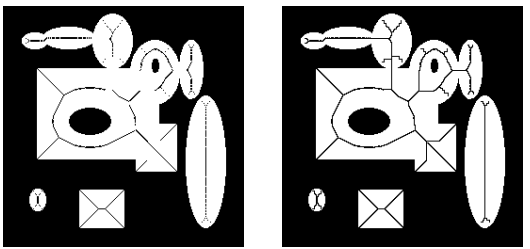

(d) (e)

Figure 13.29: Performance of Vincent's quick skeleton by maximal balls algorithm. (a) Original binary image. (b) Distance function (to be explained later). (c) Distance function visualized by contouring. (d) Non-continuous skeleton by maximal balls. (e) Final skeleton.

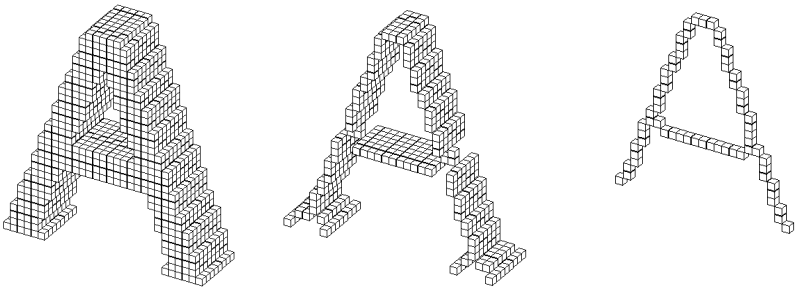

(a) (b) (c)

Figure 13.30: Morphological thinning in 3D. (a) Original 3D data set, a character A. (b) Thinning performed in one direction. (c) One voxel thick skeleton obtained by thinning image (b) in second direction. *Courtesy of K. Palágyi, University of Szeged, Hungary.*

13.5.4 Quench function, ultimate erosion

- binary point set X can be described using maximal balls B
- every point p of skeleton $S(X)$ by maximal balls has an associated ball of radius $q_X(p)$
- **quench function** used for this association
- quench function permits reconstruction of the original set X completely as union of its maximal balls B

$$X = \bigcup_{p \in S(X)} \left(p + q_X(p)B\right). \tag{13.52}$$

- $\Rightarrow$ lossless compression of a binary image.
- **global maximum** – pixel with highest value (lightest pixel, highest summit in the countryside)
- **global minimum** – deepest chasm in the countryside
- pixel p of gray-scale image is **local maximum**
  iff for every neighbor q of p, $I(p) \geq I(q)$

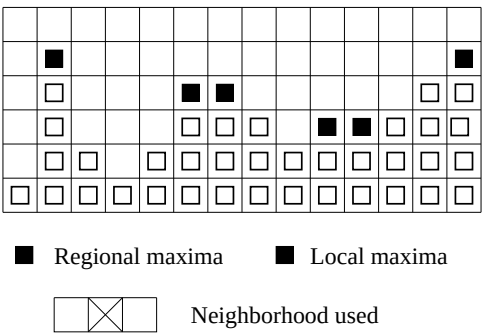

Figure 13.31: 1D illustration of regional and local maxima.

- **regional maximum** M of gray-scale image I = connected set of pixels with associated value h (plateau at altitude h), such that every neighboring pixel of M has strictly lower value than h
- ... no connected path leading upwards from a regional maximum
- if M is a regional maximum of I and $p \in M$, then p is a local maximum
- converse does not hold
- quench function is useful to define **ultimate erosion**
- often used as marker of convex objects in binary images
- **ultimate erosion** $\mathrm{Ult}(X)$ of set X = set of regional maxima of quench function
- centers of the largest maximal balls ... natural markers
- ... but ... what if objects are overlapping?
- ultimate erosion helps
- let set X consist of two overlapping disks
- skeleton is a line segment between the centers
- associated quench function has regional maxima at disk centers
- these maxima = ultimate erosion
- can be used as markers of overlapping objects

- ultimate erosion extracts one marker per object of a given shape, even if objects overlap
- but ... some objects are still multiply marked

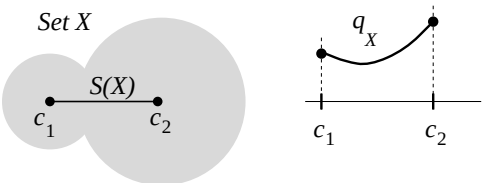

Figure 13.32: Skeleton of a set X, and associated quench function $q_X(p)$. Regional maxima give the ultimate erosion.

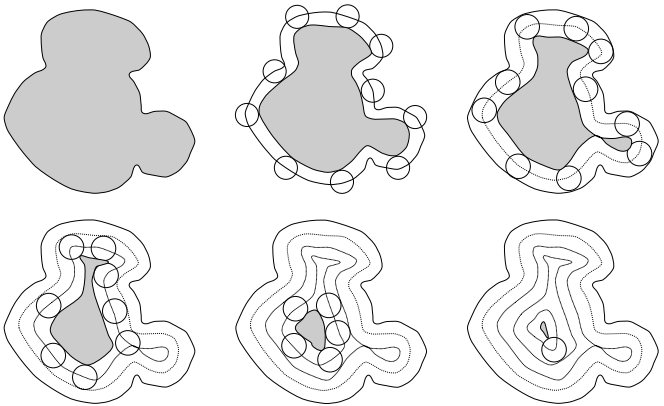

Figure 13.33: When successively eroded, the components are first separated from the rest and finally disappear from the image. The union of residua just before disappearance gives ultimate erosion.

- three rounded overlapping components of different size
- iteratively eroding the set by a unit-size ball
  shrinks
  separates
  disappears
- during successive erosions, residuals of connected components (just before they disappear) are stored
- their union is the ultimate erosion of the original set X (Figure 13.34)

13.5.5 Ultimate erosion and distance functions

- **morphological reconstruction**
- assume two sets $B \subseteq A$
- reconstruction $\rho_A(B)$ of set A from set B is union of connected components of A with non-empty intersection with B (Figure 13.35)
- (set A consists of two components)
- B may typically consist of markers that permit the reconstruction of the required part of the set A.
- Markers point to the pixel or small region that belongs to the object

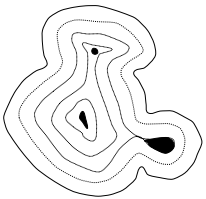

Figure 13.34: Ultimate erosion is the union of residual connected components before they disappear during erosions.

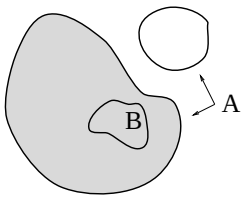

Figure 13.35: Reconstruction $\rho_A(B)$ (in gray) of the set A from the set B. Notice that set A may consist of more than one connected component.

- Ultimate erosion can be expressed

$$\mathrm{Ult}(X) = \bigcup_{n \in \mathcal{N}} \Big((X \ominus nB) \setminus \rho_{X \ominus nB}\big(X \ominus (n+1)B\big) \Big) . \tag{13.53}$$

- computationally effective ultimate erosion algorithm uses distance function
- **distance function** $\mathrm{dist}_X(p)$ is the size of the first erosion of X that does not contain p, i.e.

$$\forall p \in X , \quad \mathrm{dist}_X(p) = \min \big\{ n \in \mathcal{N},\ p \text{ not in } (X \ominus nB) \big\} . \tag{13.54}$$

- $\mathrm{dist}_X(p)$ is the shortest distance between the pixel p and background X^C

two direct applications of distance function

- ultimate erosion of set X corresponds to the union of the regional maxima of the distance function of X
- skeleton by maximal balls of set X corresponds to set of local maxima of the distance function of X

- **skeleton by influence zones** (**SKIZ**)
- let X be composed of n connected components X_i, $i = 1, \ldots, n$
- influence zone $Z(X_i)$ consists of points which are closer to set X_i than to any other connected component of X

$$Z(X_i) = \left\{ p \in \mathcal{Z}^2,\ \forall i \neq j,\ d(p, X_i) \leq d(p, X_j) \right\}. \tag{13.55}$$

- SKIZ(X) is the set of boundaries of influence zones $\left\{ Z(X_i) \right\}$

13.5.6 Geodesic transformations

Geodesic methods [**?**] modify morphological transformations to operate only on some part of an image. For instance, if an object is to be reconstructed from a marker, say a nucleus of a cell, it is desirable to avoid growing from a marker outside the cell. Another important advantage of geodesic transformations is that the structuring element can vary at each pixel, according to the image.

The basic concept of geodesic methods in morphology is geodesic distance. The path between two points is constrained within some set. The term has its roots in an old discipline—geodesy—that measures distances on the Earth's surface. Suppose that a traveler seeks the distance between London and Tokyo—the shortest distance passes *through* the Earth, but obviously the geodesic distance that is of interest to the traveler is constrained to the Earth's surface.

The **geodesic distance** $d_X(x, y)$ is the shortest path between two points x, y while this path remains entirely contained in the set X. If there is no path connecting points x, y, we set the geodesic distance $d_X(x, y) = +\infty$. Geodesic distance is illustrated in Figure 13.36.

The geodesic ball is the ball constrained by some set X. The **geodesic ball** $B_X(p, n)$ of center $p \in X$ and radius n is defined as

$$B_X(p, n) = \left\{ p' \in X,\ d_X(p, p') \leq n \right\}. \tag{13.56}$$

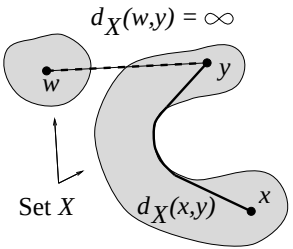

Figure 13.36: Geodesic distance $d_X(x, y)$.

The existence of a geodesic ball permits dilation or erosion only within some subset of the image; this leads to definitions of geodetic dilations and erosions of a subset Y of X.

The **geodesic dilation** $\delta_X^{(n)}$ of size n of a set Y inside the set X is defined as

$$\delta_X^{(n)}(Y) = \bigcup_{p \in Y} B_X(p, n) = \left\{ p' \in X,\ \exists p \in Y,\ d_X(p, p') \leq n \right\}. \tag{13.57}$$

Similarly the dual operation of **geodesic erosion** $\epsilon_X^{(n)}(Y)$ of size n of a set Y inside the set X can be written as

$$\epsilon_X^{(n)}(Y) = \left\{ p \in Y,\ B_X(p, n) \subseteq Y \right\} = \left\{ p \in Y,\ \forall p' \in X \setminus Y,\ d_X(p, p') > n \right\}. \tag{13.58}$$

Geodesic dilation and erosion are illustrated in Figure 13.37.

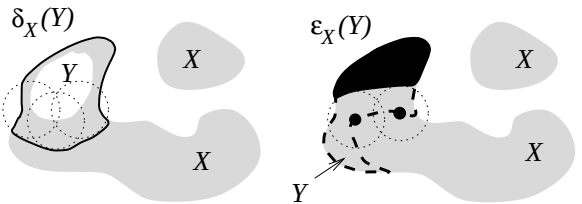

Figure 13.37: Illustration of geodesic dilation (left) and erosion (right) of the set Y inside the set X.

The outcome of a geodesic operation on a set $Y \subseteq X$ is always included within the set X. Regarding implementation, the simplest geodesic dilation of size 1 ($\delta_X^{(1)}$) of a set Y inside X is obtained as the intersection of the unit-size dilation of Y (with respect to the unit ball B) with the set X

$$\delta_X^{(1)} = (Y \oplus B) \cap X \,. \tag{13.59}$$

Larger geodesic dilations are obtained by iteratively composing unit dilations n times

$$\delta_X^{(n)} = \underbrace{\delta_X^{(1)}\Big(\delta_X^{(1)}\big(\delta_X^{(1)} \ldots (\delta_X^{(1)})\big)\Big)}_{n\ times} \,. \tag{13.60}$$

The fast iterative way to calculate geodesic erosion is similar.

13.5.7 Morphological reconstruction

Assume that we want to reconstruct objects of a given shape from a binary image that was originally obtained by thresholding. All connected components in the input image constitute the set X. However, only some of the connected components were marked by markers that represent the set Y. This task and its desired result are shown in Figure 13.38.

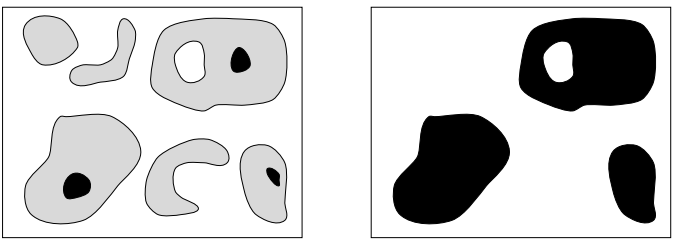

Figure 13.38: Reconstruction of X (shown in light gray) from markers Y (black). The reconstructed result is shown in black on the right side.

Successive geodesic dilations of the set Y inside the set X enable the reconstruction of the connected components of X that were initially marked by Y. When dilating from the marker, it is impossible to intersect a connected component of X which did not initially contain a marker Y; such components disappear.

Geodesic dilations terminate when all connected components set X previously marked by Y are reconstructed, i.e., idempotency is reached

$$\forall n > n_0,\ \delta_X^{(n)}(Y) = \delta_X^{(n_0)}(Y)\,. \tag{13.61}$$

This operation is called **reconstruction** and denoted by $\rho_X(Y)$. Formally

$$\rho_X(Y) = \lim_{n\to\infty} \delta_X^{(n)}(Y)\,. \tag{13.62}$$

In some applications it is desirable that one connected component of X is marked by several markers Y. If it is not acceptable for the sets grown from various markers to become connected, the notion of influence zones can be generalized to **geodesic influence zones** of the connected components of set Y inside X. The idea is illustrated in Figure 13.39.

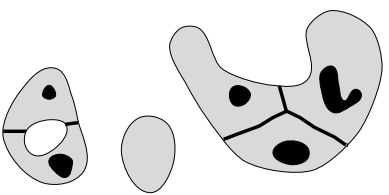

Figure 13.39: Geodesic influence zones.

We are now ready to generalize the reconstruction to gray-scale images; this requires the extension of geodesy to gray-scale images. The core of the extension is

the statement (which is valid for discrete images) that any increasing transformation defined for binary images can be extended to gray-level images [Serra 82]. By this transformation we mean a transformation Ψ such that

$$\forall X,\ Y \subset \mathcal{Z}^2,\ Y \subseteq X \Longrightarrow \Psi(Y) \subseteq \Psi(X)\,. \tag{13.63}$$

The generalization of transformation Ψ is achieved by viewing a gray-level image I as a stack of binary images obtained by successive thresholding—this is called the threshold decomposition of image I [**?**]. Let D_I be the domain of the image I, and the gray values of image I be in $\{0, 1, \ldots, N\}$. The thresholded images $T_k(I)$ are

$$T_k(I) = \Big\{ p \in D_I,\ I(P) \geq k \Big\}\,, \quad k = 0, \ldots, N\,. \tag{13.64}$$

The idea of threshold decomposition is illustrated in Figure 13.40.

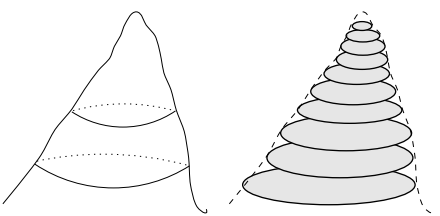

Figure 13.40: Threshold decomposition of a gray-scale image.

Threshold-decomposed images $T_k(I)$ obey the inclusion relation

$$\forall k \in [1, N],\ T_k(I) \subseteq T_{k-1}(I)\,. \tag{13.65}$$

Consider the increasing transformation Ψ applied to each threshold-decomposed image; their inclusion relationship is kept. The transformation Ψ can be extended to gray-scale images using the following **threshold decomposition principle**:

$$\forall p \in D_I,\ \Psi(I)(p) = \max\left\{k \in [0, \ldots, N],\ p \in \Psi(T_k(I))\right\}. \tag{13.66}$$

Returning to the reconstruction transformation, the binary geodesic reconstruction ρ is an increasing transformation, as it satisfies

$$Y_1 \subseteq Y_2,\ X_1 \subseteq X_2,\ Y_1 \subseteq X_1,\ Y_2 \subseteq X_2 \Longrightarrow \rho_{X_1}(Y_1) \subseteq \rho_{X_2}(Y_2). \tag{13.67}$$

We are ready to generalize binary reconstruction to **gray-level reconstruction** applying the threshold decomposition principle (13.66). Let J, I be two gray-scale images defined on the same domain D, with gray-level values from the discrete interval $[0, 1, \ldots, N]$. If, for each pixel $p \in D$, $J(p) \leq I(p)$, the gray-scale reconstruction $\rho_I(J)$ of image I from image J is given by

$$\forall p \in D,\ \rho_I(J)(p) = \max\left\{k \in [0, N],\ p \in \rho_{T_k}(T_K(J))\right\}. \tag{13.68}$$

Recall that binary reconstruction grows those connected components of the mask which are marked. The gray-scale reconstruction extracts peaks of the mask I that are marked by J (see Figure 13.41).

The duality between dilation and erosion permits the expression of gray-scale reconstruction using erosion.

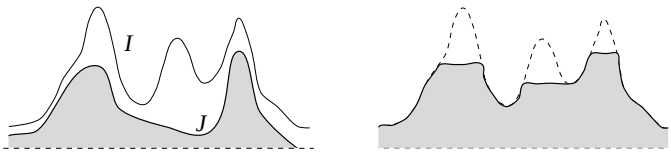

Figure 13.41: Gray-scale reconstruction of mask I from marker J.

13.6 Granulometry

Granulometry was introduced by stereologists (mathematicians attempting to understand 3D shape from cross sections)—the name comes from the Latin *granulum*, meaning grain. Matheron [**?**] used it as a tool for studying porous materials, where the distribution of pore sizes was quantified by a sequence of openings of increasing size. Currently, granulometry is an important tool of mathematical morphology, particularly in material science and biology applications. The main advantage is that granulometry permits the extraction of shape information without a priori segmentation.

Consider first a **sieving analysis** analogy; assume that the input is a heap of stones (or granules) of different sizes. The task is to analyze how many stones in the heap fit into several size classes. Such a task is solved by sieving using several sieves with increasing sizes of holes in the mesh. The result of analysis is a discrete function; on its horizontal axis are increasing sizes of stones and on its vertical axis

the numbers of stones of that size. In morphological granulometry, this function is called a **granulometric spectrum** or **granulometric curve**.

In binary morphology, the task is to calculate a granulometric curve where the independent variable is the size of objects in the image. The value of the granulometric curve is the number of objects of given size in the image. The most common approach is that sieves with increasing hole sizes (as in the example) are replaced by a sequence of openings with structural elements of increasing size.

Granulometry plays a very significant role in mathematical morphology that is analogous to the role of frequency analysis in image processing or signal analysis. Recall that frequency analysis expands the signal into a linear combination of harmonic signals of growing frequency. The **frequency spectrum** provides the contribution of individual harmonic signals—it is clear that the granulometric curve (spectrum) is analogous to a frequency spectrum.

Let $\Psi = (\psi_\lambda)$, $\lambda \geq 0$, be a family of transformations depending on a parameter λ. This family constitutes a **granulometry** if and only if the following properties of the transformation ψ hold:

$$\begin{aligned} \forall \lambda \geq 0 \quad & \psi_\lambda \text{ is increasing,} \\ & \psi_\lambda \text{ is anti-extensive,} \\ \forall \lambda \geq 0,\ \mu \geq 0 \quad & \psi_\lambda \, \psi_\mu = \psi_\mu \, \psi_\lambda = \psi_{\max(\lambda\mu)} \, . \end{aligned} \tag{13.69}$$

The consequence of property (13.69) is that for every $\lambda \geq 0$ the transformation ϕ_λ is idempotent. (ψ_λ), $\lambda \geq 0$ is a decreasing family of openings (more precisely, algebraic

openings [Serra 82] that generalize the notion of opening presented earlier). It can be shown that for any convex structuring element B, the **family of openings** with respect to $\lambda B = \{\lambda b,\ b \in B\}$, $\lambda \geq 0$, constitutes a granulometry [Matheron 75].

Consider more intuitive granulometry acting on discrete binary images (i.e., sets). Here the granulometry is a sequence of openings ψ_n indexed by an integer $n \geq 0$—each opening result is smaller than the previous one. Recall the analogy with sieving analysis; each opening, which corresponds to one sieve mesh size, removes from the image more than the previous one. Finally, the empty set is reached. Each sieving step is characterized by some measure $m(X)$ of the set (image) X (e.g., number of pixels in a 2D image, or volume in 3D). The rate at which the set is sieved characterizes the set. The pattern spectrum provides such a characteristic.

The **pattern spectrum**, also called **granulometric curve**, of a set X with respect to the granulometry $\Psi = \psi_n$, $n \geq 0$ is the mapping

$$PS_\Psi(X)(n) = m[\psi_n(X)] - m[\psi_{n-1}(X)]\,, \quad \forall n > 0\,. \tag{13.70}$$

The sequence of openings $\Psi(X)$, $n \geq 0$ is a decreasing sequence of sets, i.e., $\big[\psi_0(X) \supseteq \psi_1(X) \supseteq \psi_2(X) \supseteq \ldots\big]$. The granulometry and granulometric curve can be used.

Suppose that the granulometric analysis with family of openings needs to be computed for a binary input image. The binary input image is converted into a gray-level image using a granulometry function $G_\Psi(X)$, and the pattern spectrum PS_Ψ is calculated as a histogram of the granulometry function.

The **granulometry function** $G_\Psi(X)$ of a binary image X from granulometry $\Psi = (\psi_n)$, $n \geq 0$, maps each pixel $x \in X$ to the size of the first n such that $x \notin \psi_n(X)$:

$$x \in X,\ G_\Psi(X)(x) = \min\left\{n > 0,\ x \notin \psi_n(X)\right\}. \tag{13.71}$$

The pattern spectrum PS_Ψ of a binary image X for granulometry $\Psi = (\psi_n)$, $n \geq 0$, can be computed from the granulometry function $G_\Psi(X)$ as its histogram

$$\forall n > 0,\ PS_\Psi(X)(n) = \text{card}\big\{p,\ G_\Psi(X)(p) = n\big\} \tag{13.72}$$

(where 'card' denotes cardinality). An example of granulometry is given in Figure 13.42. The input binary image with circles of different radii is shown in Figure 13.42a; Figure 13.42b shows one of the openings with a square structuring element. Figure 13.42c illustrates the granulometric power spectrum. At a coarse scale, three most significant signals in the power spectrum indicate three prevalent sizes of object. The less significant signals on the left side are caused by the artifacts that occur due to discretization. The Euclidean circles have to be replaced by digital entities (squares).

We see in this example that granulometries extract size information without the need to identify (segment) each object a priori. In applications, this is used for shape description, feature extraction, texture classification, and removal of noise introduced by image borders.

Until recently, granulometric analysis using a family of openings was too slow to be practically useful, but recent developments have made granulometries quick

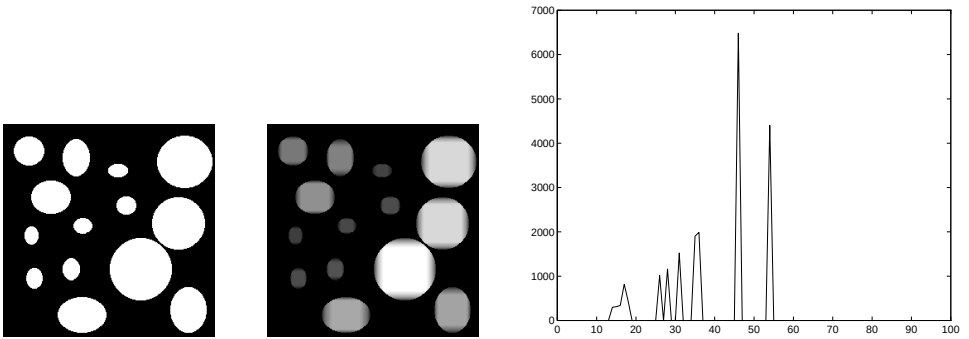

(a) (b) (c)

Figure 13.42: Example of binary granulometry performance. (a) Original binary image. (b) Maximal square probes inscribed—the initial probe size was 2×2 pixels. (c) Granulometric power spectrum as histogram of (b)—the horizontal axis gives the size of the object and the vertical axis the number of pixels in an object of given size. *Courtesy of P. Kodl, Rockwell Automation Research Center, Prague, Czech Republic.*

and useful; the reader interested in implementation may consult [**?** **?**]. For binary images, the basic idea towards speed-up is to use linear structuring elements for openings and more complex 2D ones derived from it, such as cross, square, or diamond (see Figure 13.43). The next source of computational saving is the fact that some 2D structuring elements can be decomposed as Minkowski addition of two 1D structuring elements. For example, the square structuring element can be expressed as Minkowski addition of horizontal and vertical lines.

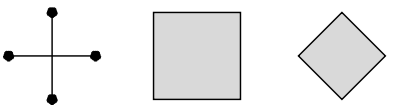

Figure 13.43: Structural elements used for fast binary granulometry are derived from line structuring elements, e.g., cross, square, and diamond.

Gray-scale granulometric analysis is another recent development that permits the extraction of size information directly from gray-level images. The interested reader should consult [**?**].

13.7 Morphological segmentation and watersheds

13.7.1 Particles segmentation, marking, and watersheds

- Mathematical morphology segments images of texture or images of particles
- input image – binary or gray-scale
- binary case – segmenting overlapping particles
- gray-scale case – object contour extraction
- two basic steps:
  1. location of particle markers
  2. watersheds used for particle reconstruction
- **marker** of object or set X is a set M that is included in X
- markers have the same homotopy as set X, and are typically located in the central part of the object (particle)
- application-specific knowledge should be used
- combinations of non-morphological and morphological approaches may be used
- when marked, objects can be grown from the markers
  e.g., using the watershed transformation

13.7.2 Binary morphological segmentation

- task: find objects that differ in brightness from uneven background
- $\Rightarrow$ top hat transformation
  finds peaks in image function that differ from the local background
  gray-level shape of the peaks does not play role
  shape of structuring element does
- Watershed segmentation considers both sources of information and supersedes top hat approach

- binary images – each particle is marked first
  (e.g., ultimate erosion may be used)
- next task: grow objects from the markers provided they are kept within the limits of the original set and parts of objects are not joined when they come close to each other
- oldest technique: **conditional dilation**
- ordinary dilation used for growing
  result is constrained by two conditions
  - remain in the original set
  - do not join particles
- **Geodesic reconstruction** – more sophisticated, much faster than conditional dilation
  structuring element adapts according to the neighborhood of the processed pixel
- **Geodesic influence zones**
  Figure 13.45 shows that the result can differ from our intuitive expectation

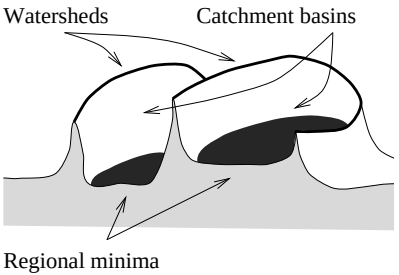

Figure 13.44: Illustration of catchment basins and watersheds in a 3D landscape view.

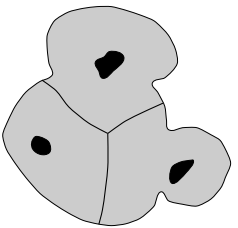

Figure 13.45: Segmentation by geodesic influence zones (SKIZ) need not lead to correct results.

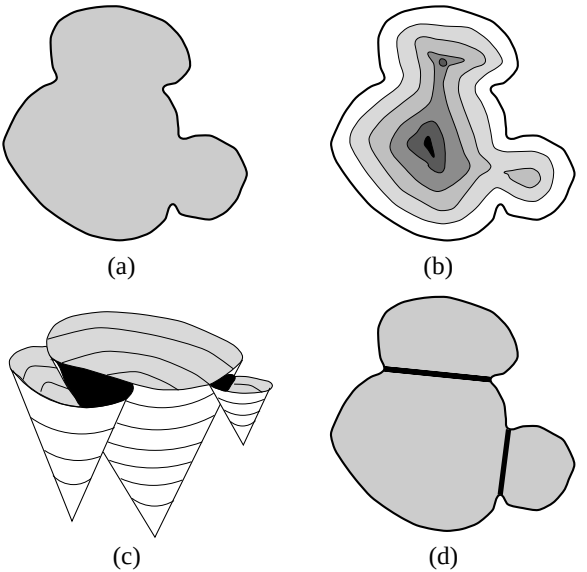

Figure 13.46: Segmentation of binary particles. (a) Input binary image. (b) Gray-scale image created from (a) using the −dist function. (c) Topographic notion of the catchment basin. (d) Correctly segmented particles using watersheds of image (b).

- **watershed transformation** – best solution
- original binary image is converted into gray-scale using negative distance transform $-\text{dist}$ (13.54).
- if drop of water falls onto a topographic surface of the $-\text{dist}$ image — follows steepest slope towards a regional minimum

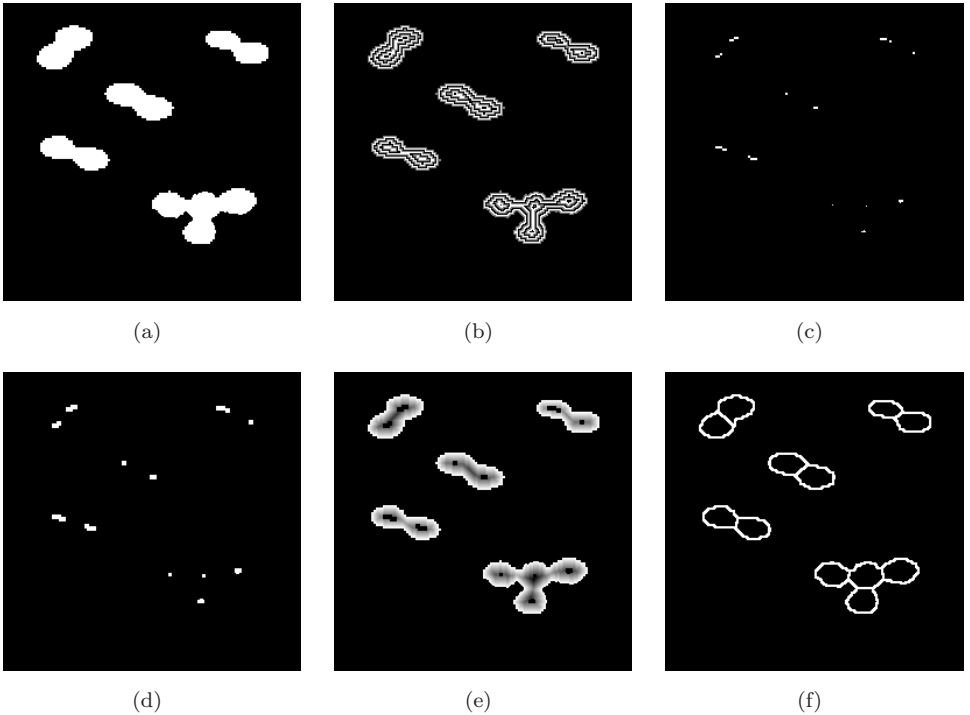

Figure 13.47: Particle segmentation by watersheds. (a) Original binary image. (b) Distance function visualized using contours. (c) Regional maxima of the distance function used as particle markers. (d) Dilated markers. (e) Inverse of the distance function with the markers superimposed. (f) Resulting contours of particles obtained by watershed segmen-

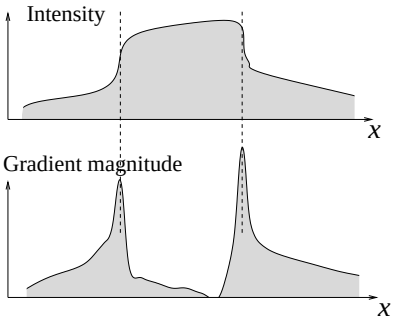

Figure 13.48: Segmentation in gray-scale images using gradient magnitude.

13.7.3 Gray-scale segmentation, watersheds

- markers and watersheds method can also be applied to gray-scale segmentation
- Watersheds are used as crest-line extractors in gray-scale images
- region contour in gray-level image == points where gray-levels change most quickly
  (analogous to edge-based segmentation)
- watershed transformation is applied to gradient magnitude image
- simple approximation to the gradient image is used in mathematical morphology

- Beucher's gradient is calculated as algebraic difference of unit-size dilation and unit-size erosion of the input image X

$$\text{grad}(X) = (X \oplus B) - (X \ominus B)\,. \tag{13.73}$$

- main problem of segmentation via gradient images without markers is **oversegmentation**
- watershed segmentation methods with markers do not suffer from oversegmentation

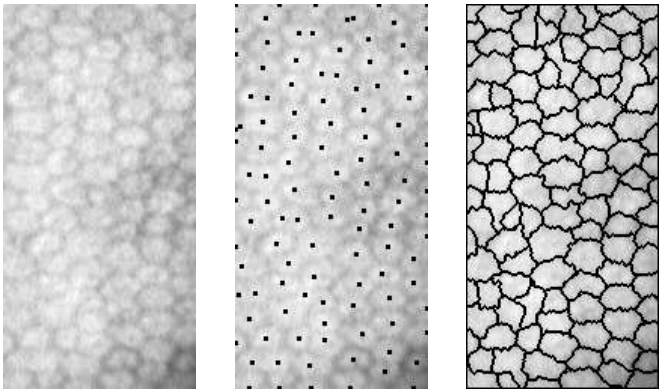

(a) (b) (c)

Figure 13.49: Watershed segmentation on the image of a human retina. (a) Original gray-scale image. (b) Dots are superimposed markers found by nonmorphological methods. (c) Boundaries of retina cells found by watersheds from markers (b). *Data and markers courtesy of R. Šára, Czech Technical University, Prague, segmentation courtesy of P. Kodl, Rockwell Automation Research Center Prague, Czech Republic.*

13.8 Summary

- **Mathematical morphology**
  - Mathematical morphology stresses the role of **shape** in image pre-processing, segmentation, and object description. It constitutes a set of tools that have a solid mathematical background and lead to fast algorithms. The basic entity is a **point set**. Morphology operates using transformations that are described using operators in a relatively simple **non-linear algebra**. Mathematical morphology constitutes a counterpart to traditional signal processing based on linear operators (such as convolution).
  - Mathematical morphology is usually divided into **binary mathematical morphology** which operates on binary images (2D point sets), and **gray-level mathematical morphology** which acts on gray-level images (3D point sets).
- **Morphological operations**
  - In images, morphological operations are **relations of two sets**. One is an image and the second a small probe, called a **structuring element**, that systematically traverses the image; its relation to the image in each position is stored in the output image.
  - Fundamental operations of mathematical morphology are **dilation** and **erosion**. Dilation expands an object to the closest pixels of the neighborhood. Erosion shrinks the object. Erosion and dilation are not invertible

operations; their combination constitutes new operations—**opening** and **closing**.

– Thin and elongated objects are often simplified using a **skeleton** that is an archetypical stick replacement of original objects. The skeleton constitutes a line that is in 'the middle of the object'.

– The **distance function** (transform) to the background constitutes a basis for many fast morphological operations. **Ultimate erosion** is often used to mark blob centers. There is an efficient **reconstruction** algorithm that grows the object from the marker to its original boundary.

– **Geodesic transformations** allow changes to the structuring element during processing and thus provide more flexibility. They provide quick and efficient algorithms for image **segmentation**. The **watershed transform** represents one of the better segmentation approaches. Boundaries of the desired regions are influence zones of regional minima (i.e., seas and lakes in the landscape). Region boundaries are watershed lines between these seas and lakes. The segmentation is often performed from **markers** chosen by a human or from some automatic procedure that takes into account semantic properties of the image.

– **Granulometry** is a quantitative tool for analyzing images with particles of different size (similar to sieving analysis). The result is a discrete **granulometric curve** (spectrum).

13.9 References

Golay 69] M J E Golay. Hexagonal parallel pattern transformation. *IEEE Transactions on Computers*, C–18:733–740, 1969.

Ma and Sonka 96] C M Ma and M Sonka. A fully parallel 3D thinning algorithm and its applications. *Computer Vision and Image Understanding*, 64:420–433, 1996.

Matheron 75] G Matheron. *Random Sets and Integral Geometry.* Wiley, New York, 1975.

Palagyi et al. 06] Kalman Palagyi, Juerg Tschirren, Eric A. Hoffman, and Milan Sonka. Quantitative analysis of pulmonary airway tree structures. *Computers in Biology and Medicine*, 36:974–996, 2006.

Serra 82] J Serra. *Image Analysis and Mathematical Morphology.* Academic Press, London, 1982.

Vincent 91] L Vincent. Efficient computation of various types of skeletons. In *Proceedings of the SPIE Symposium Medical Imaging,* San Jose, CA, volume 1445, SPIE, Bellingham, WA, 1991.